

# CEILING JET FLOWS

David D. Evans

## INTRODUCTION

Much of the hardware associated with detection and suppression of fires in commercial, manufacturing, storage, and recently constructed residential buildings is located near the ceiling surfaces. In the event of a fire, hot gases in the fire plume rise directly above the burning fuel and impinge on the ceiling. The ceiling surface causes the flow to turn and move horizontally under the ceiling to other areas of the building remote from the fire position. The response of smoke detectors, heat detectors, and sprinklers installed below the ceiling so as to be submerged in this hot flow of combustion products from a fire provides the basis for the building fire protection.

Studies quantifying the flow of hot gases under a ceiling resulting from the impingement of a fire plume have been conducted since the 1950s. Early studies at the Fire Research Station in Great Britain,<sup>1,2</sup> and more recently at Factory Mutual Research Corporation,<sup>3-6</sup> the National Institute of Standards and Technology (NIST),<sup>7,8</sup> and at other research laboratories,<sup>9,10</sup> have sought to quantify the gas temperatures and velocities in the hottest portion of the flow produced by steady fires beneath smooth, unconfined horizontal ceilings.

"Ceiling jet" refers to the relatively rapid gas flow in a shallow layer beneath the ceiling surface which is driven by the buoyancy of the hot combustion products. Figure 2-4.1 shows an idealization of the ceiling jet flow beneath an unconfined ceiling. In actual fires within buildings, the simple conditions pictured—a hot rapidly moving gas layer between the ceiling surface and the tranquil ambient air at room temperature—exist only at the beginning of a fire when the quantity of hot gases produced is not sufficient to accumulate into a stagnant warm gas layer in the upper portion of the compartment. The accumulation of this warm gas layer can be retarded by venting the ceiling jet flow through openings in the ceiling surface or edges. As shown in Figure 2-4.1, the ceiling jet flow emerges from the region of plume im-

pingement on the ceiling, flowing away from the fire. As it does, the layer grows thicker by entraining room air at the lower boundary. This entrained air cools the gases in the jet and reduces its velocity. As the hot gases move out across the ceiling, the portion adjacent to the ceiling surface is cooled by heat transfer.

Quantification of the heat transfer from fire plumes impinging on ceiling surfaces is an area of recent research activity.<sup>7-11</sup> As a rule of thumb,<sup>3</sup> the thickness of the ceiling jet flow is 5 to 12 percent of the ceiling-to-fire-source height. Within this ceiling jet flow, the maximum temperature and velocity occurs within 1 percent of the distance from the ceiling to the fire source.<sup>3</sup> Detailed measurement and analysis of the temperature and velocity distributions in the ceiling jet flow for the region  $r/H < 2$  has been performed by Motevalli and Marks.<sup>12</sup>

Much of the work that is collected below deals with means to predict the temperature and velocities in the ceiling jet flow both above and remote from the fire source. In most cases, the reported information deals only with predictions of the maximum temperature and velocity in the flow at positions normally one percent of the fire-source distance below the ceiling. Often fire detectors or sprinklers are placed at ceiling standoff distances which are outside of this region and therefore will experience cooler temperatures and lower velocities than predicted. In facilities with very high ceilings, the detectors could be closer to the ceiling than one percent of the ceiling-to-fire-source separation and will fall in the ceiling jet thermal and viscous boundary layers. In low-ceiling facilities, it is possible for sprinklers or detectors to be placed outside of the ceiling jet flow entirely if the standoff is greater than 12 percent of the ceiling-to-fire-source height. In this case response time could be drastically increased.

## STEADY FIRES

A generalized theory to predict gas velocities, gas temperatures, and the depth of steady fire-driven ceiling jet flows has been developed by Alpert.<sup>4</sup> This work involved the use of several idealizations in the construction of the theoretical model, but results are likely to provide reasonable estimates over radial distances of one or two ceiling heights from the point of fire plume impingement on the ceiling.

Dr. David D. Evans is the acting-chief of the Fire Safety Engineering Division at the National Institute of Standards and Technology, Building and Fire Research Laboratory. He is engaged in research to support the development of performance-based fire standards and means to predict and mitigate the impact of large fires.

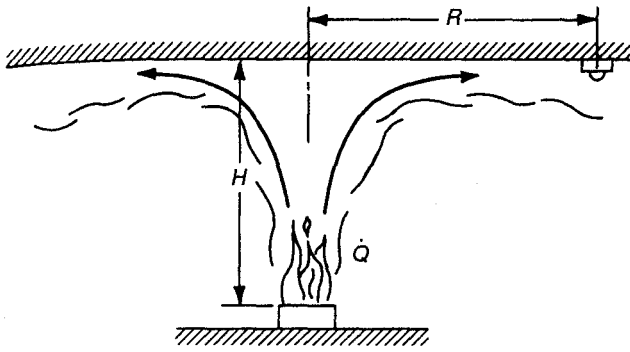


Fig. 2-4.1. Ceiling jet flow beneath an unconfined ceiling.

Alpert<sup>3</sup> has also developed easy-to-use correlations to quantify the maximum gas temperature and velocity at a given position in a ceiling jet flow produced by a steady fire. These correlations are widely used in hazard analysis calculations. They have been employed by Evans and Stroup<sup>13</sup> in the development of a generalized program for prediction of heat detector response for the case of the detector totally submerged in the ceiling jet flow. The correlations are based on measurements collected during test burns of fuel arrays of wood and plastic pallets, cardboard boxes, plastic materials in cardboard boxes, and liquid fuels with energy release rates ranging from 668 kW to 98 MW under ceiling heights from 4.6 to 15.5 m. The correlations developed by Alpert<sup>3</sup> for determining maximum ceiling jet temperatures and velocities in S.I. units are

$$T - T_{\infty} = \frac{16.9\dot{Q}^{2/3}}{H^{5/3}} \quad \text{for } r/H \leq 0.18 \quad (1)$$

$$T - T_{\infty} = \frac{5.38(\dot{Q}/r)^{2/3}}{H} \quad \text{for } r/H > 0.18 \quad (2)$$

$$U = 0.96\left(\frac{\dot{Q}}{H}\right)^{1/3} \quad \text{for } r/H \leq 0.15 \quad (3)$$

$$U = \frac{0.195\dot{Q}^{1/3}H^{1/2}}{r^{5/6}} \quad \text{for } r/H > 0.15 \quad (4)$$

where temperature,  $T$ , is in °C; velocity,  $U$ , is in m/s; and total energy release rate,  $\dot{Q}$ , is in kW; and ceiling height and radial position ( $r$  and  $H$ ) are in m.

Data from these tests were correlated using the total energy release rate of the fire. Even though it is the convective fraction of the total energy release rate that is directly related to the buoyancy of the fire, most available data is correlated using the total energy release rate. For common materials, such as those used by Alpert, the convective energy release rate,  $\dot{Q}_c$ , is considered to be proportional to the total energy release rate,  $\dot{Q}$ .

The correlations for both temperatures and velocities (Equations 1 through 4) are broken into two parts. One part applies for the ceiling jet in the area of the impingement point where the upward flow of gas in the plume turns to flow out beneath the ceiling horizontally. These correlations (Equations 1 and 3) are independent of radius and are actually axial plume flow temperatures and velocities calculated at the ceiling height above the fire source. The other corre-

lations apply outside of this turning region as the flow moves away from the impingement area. Certain constraints should be understood when applying these correlations in the analysis of fire flows. The correlations apply only during times after fire ignition when the ceiling flow may be considered unconfined; i.e., no accumulated warm upper layer is present. Walls close to the fire affect the temperatures and velocity in the ceiling jet. The correlations were developed from test data to apply in cases where the fire source is at least a distance 1.8 times the ceiling height from the enclosure walls. Ideally, for the special cases where burning fuel is located against wall surfaces or two wall surfaces forming a 90-degree corner, the correlations may be adjusted based on method of reflection making use of symmetry to account for the effects of the walls blocking entrainment of air into the fire plume. For the case of a fire adjacent to a flat wall,  $2\dot{Q}$  is substituted for  $\dot{Q}$  in the correlations. For a fire in a 90-degree corner,  $4\dot{Q}$  is substituted for  $\dot{Q}$  in the correlations.<sup>3</sup>

Experiments have shown that, unless great care is taken to ensure that the fuel perimeter is in contact with the wall surfaces, the method of reflection used to estimate the effects of the walls on ceiling jet temperature will be inaccurate. For example, Zukoski *et al*<sup>14</sup> found that a circular burner placed against a wall so that only one point on the perimeter contacted the wall, behaved almost identically to a fire far from the wall with plume entrainment only decreasing by 3 percent. When using Equations 1 through 4, this fire would be represented by replacing  $\dot{Q}$  with  $1.05\dot{Q}$  and not  $2\dot{Q}$  as would be predicted by the method of reflections. The value of  $2\dot{Q}$  would be appropriate for a semicircular burner with the entire flat side pushed against the wall surface.

Consider the following calculations, which demonstrate typical uses of the correlations, using Equations 1 through 4.

- (a) The maximum temperature rise under a ceiling 10 m directly above a 1.0 MW energy release rate fire is calculated using Equation 1 as

$$\begin{aligned} T - T_{\infty} &= \frac{16.9(1000)^{2/3}}{10^{5/3}} \\ &= \frac{16.9(100)}{46.42} \end{aligned}$$

$$\Delta T = 36.4^{\circ}\text{C}$$

- (b) The minimum energy release rate of a fire against non-combustible walls in the corner of a building 12 m below the ceiling needed to raise the temperature of the gas below the ceiling 50°C at a distance 5 m from the corner is calculated using Equation 2 and the symmetry substitution of  $4\dot{Q}$  for  $\dot{Q}$  to account for the effects of the corner as

$$T - T_{\infty} = \frac{5.38(4\dot{Q}/r)^{2/3}}{H}$$

$$50 = \frac{5.38(4\dot{Q}/5)^{2/3}}{12}$$

$$\dot{Q} = \frac{5}{4} \left[ \frac{50(12)}{5.38} \right]^{3/2}$$

$$\dot{Q} = 1472 \text{ kW}$$

$$\dot{Q} = 1.472 \text{ MW}$$

- (c) The maximum velocity at this position is calculated from Equation 4, modified to account for the effects of the corner as

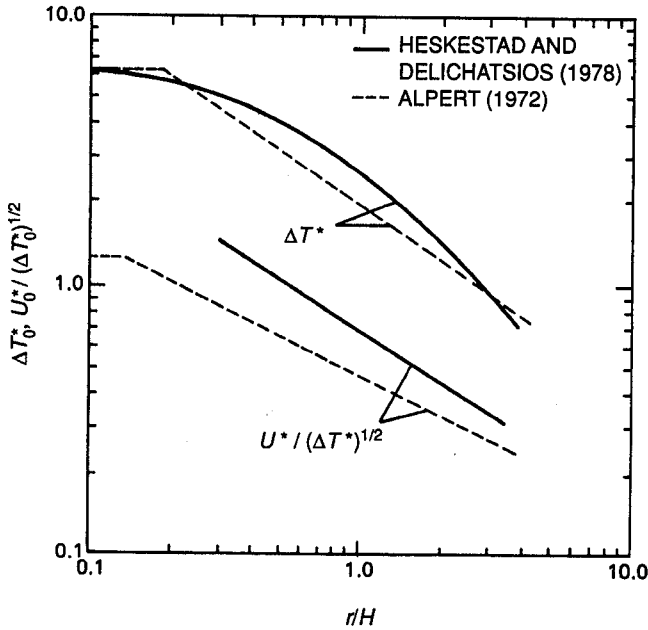


Fig. 2-4.2. Dimensionless correlations for maximum ceiling jet temperatures and velocities produced by steady fires. Solid line: Heskestad and Delichatsios<sup>15</sup>; dotted line: Alpert.<sup>3</sup>

$$U = \frac{0.197(4\dot{Q})^{1/3}H^{1/2}}{r^{5/6}}$$

$$= \frac{0.197(5888)^{1/3}(12)^{1/2}}{5^{5/6}}$$

$$U = 3.2 \text{ m/s}$$

Heskestad and Delichatsios<sup>15</sup> have developed correlations for maximum ceiling jet temperature rise and velocities that are based on testing completed subsequent to Alpert's analysis.<sup>3</sup> Their correlations are cast in generalized variables (indicated by the superscript asterisk) for energy release rate, temperature rise, and velocity as

$$\dot{Q}_0^* = \dot{Q}/(\rho_\infty c_p T_\infty g^{1/2} H^{5/2}) \quad (5)$$

$$\Delta T_0^* = \Delta T/T_\infty / (\dot{Q}_0^*)^{2/3} = [0.188 + 0.313r/H]^{-4/3} \quad (6)$$

$$U_0^* = 0.68(\Delta T_0^*)^{1/2}(r/H)^{-0.63} \quad \text{for } r/H \geq 0.3 \quad (7)$$

For the case of steady fires under unconfined ceilings, Figure 2-4.2 shows the plot of the Heskestad and Delichatsios correlation for temperature rise and velocity as solid line curves. The correlations developed by Alpert are plotted as broken curves, using the same dimensionless parameters with assumed ambient temperature of 293 K (20°C), normal atmospheric pressure, and convective energy release rate equal to the total energy release rate,  $\dot{Q}_c = \dot{Q}$ . Generally, the results of Heskestad and Delichatsios predict larger temperature rises and gas velocities than Alpert's results.

Other methods used to calculate estimates of ceiling jet velocity distributions and maximum possible (adiabatic) ceiling jet temperatures are reported by Cooper and Woodhouse.<sup>8</sup> A recent review of ceiling jet correlations for temperature rise and velocity has been assembled by Beyler.<sup>16</sup>

## TIME DEPENDENT FIRES

For time dependent fires, all estimates from the previous section may still be used, but with the constant energy release rate,  $\dot{Q}$ , replaced by an appropriate time dependent  $\dot{Q}(t)$ . In making this replacement, a "quasisteady" flow has been assumed. This assumption implies that when a change in energy release rate occurs at the fire source, its full effects are felt everywhere in the flow field immediately. In a relatively small room-size enclosure, under conditions where the fire is growing slowly, this assumption is reasonable. In large industrial facilities, where travel times of the fire gases from the burning fuel to a detector or sprinkler submerged in the ceiling jet flow may be 10 s or longer, this may not be an appropriate assumption, depending largely on the rate of fire growth and desired accuracy of the gas temperature and velocity predictions.

Testing has shown that the energy release rate during the growth phase of many fires can often be characterized by simple time dependent polynomial or exponential functions. The most extensive research and analysis have been performed with energy release rates that vary with the second power of time.

### $t^2$ Fire Growth

The growth phase of many fires can be characterized as increasing proportionally with the square of time, measured from an ignition reference time,  $t_i$ , as

$$\dot{Q} = \alpha(t - t_i)^2 \quad (8)$$

Figure 2-4.3 shows one case where the energy release rate for a burning foam sofa during the growth phase of the fire more than 80 seconds ( $t_i$ ) after ignition<sup>17</sup> can be represented by the equation

$$\dot{Q} = 0.1736(t - 80)^2 \quad (9)$$

In an extensive series of tests conducted by Factory Mutual Research Corporation,<sup>15,18</sup> measurements were made of maximum ceiling jet temperatures and velocities during the growth of fires in which various wood cribs were burned. The energy release rate,  $\dot{Q}$ , from these fires was calculated as the product of measured mass loss rate and oxygen bomb calorimeter values for the heat of combustion

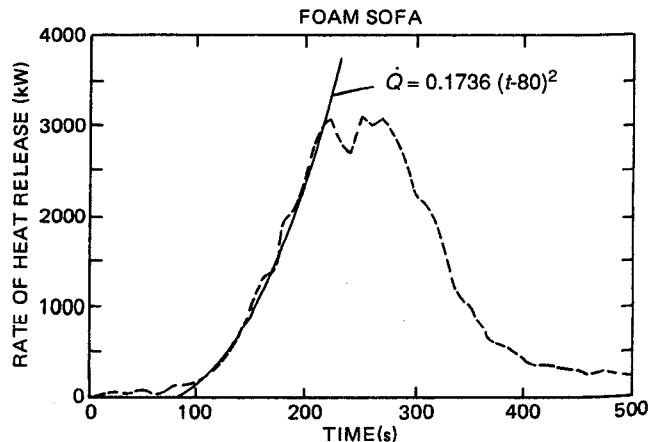


Fig. 2-4.3. Energy release rate history for a burning foam sofa.<sup>17</sup>

of the wood, which was found to be 20.9 MJ/kg. The resulting dimensionless correlations for maximum ceiling jet temperatures and velocities are

$$\Delta T_2^* = \begin{cases} 0, & t^* \leq t_f^* \\ \left( \frac{t_2^* - t_f^*}{0.188 + 0.313 r/H} \right)^{4/3} & t^* > t_f^* \end{cases} \quad (10a) \quad (10b)$$

$$U_2^* / \sqrt{\Delta T_2^*} = 0.59(r/H)^{-0.63} \quad (11)$$

where

$$t_2^* = (t - t_i) / (A^{-1/5} \alpha^{-1/5} H^{4/5}) \quad (12)$$

$$U_2^* = U / (A^{1/5} \alpha^{1/5} H^{1/5}) \quad (13)$$

$$\Delta T_2^* = (T - T_\infty) / [A^{2/5} (T_\infty/g) \alpha^{2/5} H^{-3/5}] \quad (14)$$

$$A = g / (c_p T_\infty \rho_\infty) \quad (15)$$

$$\alpha = \dot{Q} / (t - t_i)^2 \quad (16)$$

$$t_f^* = 0.954(1 + r/H) \quad (17)$$

where dimensionless variables are indicated with the superscript asterisk. Notice that in Equation 10b the dimensionless time,  $t_2^*$ , has been reduced by the time  $t_f^*$ . This reduction accounts for the gas travel time between the fire source and the location of interest along the ceiling at the specified  $r/H$ .

The dimensional temperature rise  $\Delta T_2$  (Equations 10b and 14) for the  $t^2$  fire growth is related to the temperature rise from the steady fire analysis,  $\Delta T_0$ , (Equation 6) by the simple relationship

$$\frac{\Delta T_2}{\Delta T_0} = \left( \frac{t - t_i - t_f}{t - t_i} \right)^{4/3} \quad (18)$$

This relationship may be used to evaluate the extent to which a quasisteady analysis of a growing  $t^2$  fire is appropriate.

These correlations of ceiling jet temperatures and velocities are the basis for the calculated values of fire detector spacing found in NFPA 72, *National Fire Alarm Code*, Appendix B, Engineering Guide for Automatic Fire Detector Spacing.<sup>19</sup> In NFPA 72, three or four selected fire energy release rates assumed to increase proportionally with the square of time were used as the basis for the evaluation. These fire energy release rate histories were chosen to be representative of actual fire situations involving different commodities and geometric storage arrangements. These idealized fire energy release rates are

$$\text{Slow,} \quad \dot{Q} = 0.00293t^2 \quad (19)$$

$$\text{Medium,} \quad \dot{Q} = 0.01172t^2 \quad (20)$$

$$\text{Fast,} \quad \dot{Q} = 0.0469t^2 \quad (21)$$

$$\text{Ultrafast,} \quad \dot{Q} = 0.1876t^2 \quad (22)$$

where  $\dot{Q}$  is in kW and  $t$  is in s. Consider the following calculation which demonstrates a use of the correlation (Equations 10b and 11) for calculation of ceiling jet maximum temperature and velocity produced by a  $t^2$  fire growth:

A foam sofa, of the type analyzed in Figure 2-4.3, is burning in a showroom 5 m below a suspended ceiling. The showroom temperature remote from the fire remains at 20°C at floor level as the fire begins to grow. Determine the gas temperature and velocity at the position of a ceiling-mounted fire detector submerged in the ceiling jet flow 4 m away from the fire axis when the fire energy release rate first reaches 2.5 MW.

Figure 2-4.3 shows that the energy release rate from the sofa first reaches 2.5 MW (2500 kW) at about 200 s after ignition. Using the analytic formula for the time dependent energy release rate, Equation 9, the time from the virtual ignition of the sofa at 80 s to reach 2500 kW is

$$2500 = 0.1736 (t - 80)^2 \\ (t - 80) = 120 \text{ s}$$

In this problem, the low-level energy release rate up to 80 s after actual ignition of the sofa is ignored. Thus, the sofa fire can be treated as having started at  $t = 80$  seconds and grown to 2.5 MW in the following 120 seconds. Equations 12 through 17 are used to evaluate parameters of the problem, using the dimensionless correlations for ceiling jet temperature and velocity.

For the sofa fire in the showroom example,  $T = 293 \text{ K}$ ,  $\rho = 1.204 \text{ kg/m}^3$ ,  $c_p = 1 \text{ kJ/kg K}$ ,  $g = 9.8 \text{ m/s}^2$ ,  $\alpha = 0.1736 \text{ kW/s}^2$ ,  $A = 0.0278 \text{ m}^4/\text{kJ s}^2$ ,  $r = 4 \text{ m}$ ,  $H = 5 \text{ m}$ ,  $t_f^* = 1.72$ ,  $t - t_i = 120 \text{ s}$ , and  $t_2^* = 11.40$ . For the conditions of interest  $t_2^* > t_f^*$ , so the correlation (Equation 10b) is used to evaluate the dimensionless ceiling jet temperature

$$\Delta T_2^* = \left[ \frac{11.40 - 1.72}{0.188 + 0.313(4/5)} \right]^{4/3} \\ \Delta T_2^* = 61.9$$

Equation 11 is used to calculate the dimensionless ceiling jet velocity

$$U_2^* = 0.59(4/5)^{-0.63}(61.9)^{1/2} \\ = 5.34$$

The dimensional temperature rise and velocity are calculated using Equations 14 and 13, respectively, to yield

$$\Delta T = 83.5 \text{ K} \\ T = 83.5 \text{ K} + 293 \text{ K} = 376.5 \text{ K} = 103.5^\circ\text{C} \\ U = 2.54 \text{ m/s}$$

## CONFINED CEILINGS

The corresponding gas temperature calculated with the quasi-steady analysis Equations 6 or 18 instead of the  $t^2$ -fire analysis is 124°C.

Previous discussions of ceiling jets in this chapter have all dealt with unconfined radial spread of the gas flow away from a ceiling impingement point. In practice this flow may be interrupted by ceiling beams or walls in a corridor situation creating a long channel that partially confines the flow. In this case, the flow near the impingement point will remain radial, but after spreading to the walls or beams that bound the ceiling, the flow will be altered into a channel flow. Delichatsios<sup>20</sup> has developed correlations for ceiling jet temperatures and velocity which apply to the channel flow between beams and down corridors. In the case of corridors,

the correlations apply when the corridor half-width,  $\ell_b$ , is greater than 0.2 times the distance from the fire source to the ceiling,  $H$ , or ( $\ell_b/H > 0.2$ ). In the case of beams, the flows must also be contained fully, so that a channel flow results without "spillage" over the beams. In order for this condition to be satisfied, the beam depth,  $h_b$ , must be greater than the quantity  $(H/10)(\ell_b/H)^{-1/3}$  or

$$h_b/H > 0.1(\ell_b/H)^{-1/3}$$

then

$$\frac{\Delta T}{\Delta T_{imp}} = 0.29 \left(\frac{H}{\ell_b}\right)^{1/3} \exp[-0.20(Y/H)(\ell_b/H)^{1/3}]$$

for  $Y > \ell_b$

where  $\Delta T_{imp}$  is the temperature in the gas near the ceiling directly over the fire, and  $Y$  is the distance along the channel measured from the plume impingement point.

Generally, for large industrial or commercial storage facilities, the analysis for unconfined ceiling jet flows will be sufficient for most purposes. In smaller rooms, or for very long times after fire ignition in larger industrial facilities, a quiescent warm layer of gas will accumulate in the upper portion of the enclosure. This warm layer can be deep enough to totally submerge the ceiling jet flow. In that case, temperatures in the ceiling jet can be expected to be greater than if the ceiling jet was entraining gas from the cooler room ambient temperature layer. Quantitative methods for the prediction of temperature and velocity in a two-layer room environment in which the ceiling jet is contained totally in a warm upper layer and the fire is burning totally in the lower cool layer have been formulated. Contributions to this area have been made by Evans,<sup>21,22</sup> Cooper,<sup>23</sup> and Zukoski and Kubota.<sup>11</sup>

In these methods, the flow of the ceiling jet within the warm upper layer of the enclosure is imagined to result from a fire totally contained in a uniform ambient environment with temperature equal to that of the warm upper layer. This substitute fire has an energy release rate,  $\dot{Q}_2$ , and location below the ceiling,  $H_2$ , differing from the original fire. Calculation of the substitute quantities  $\dot{Q}_2$  and  $H_2$  depends on the energy release rate and location of the original fire as well as the depths and temperatures of the upper and lower layers within the enclosure.

Following the development by Evans,<sup>22</sup> the substitute source energy release rate and distance below the ceiling are calculated from Equations 23 through 26. Originally developed for the purpose of sprinkler and heat detector response time calculations, these equations are applicable during the growth phase of enclosure fires.

$$\dot{Q}_{I,2}^* = [(1 + C_T \dot{Q}_{I,1}^{*2/3})/\xi C_T - 1/C_T]^{3/2} \quad (23)$$

$$Z_{I,2} = \left\{ \frac{\xi \dot{Q}_{I,1}^* C_T}{\dot{Q}_{I,2}^{*1/3} [(\xi - 1)(\beta^2 + 1) + \xi C_T \dot{Q}_{I,2}^{*2/3}]} \right\}^{2/5} Z_{I,1} \quad (24)$$

$$\dot{Q}_{c,2} = \dot{Q}_{I,2}^* \rho_{\infty,2} c_{p\infty} T_{\infty,2} \beta^{5/2} Z_{I,2}^{5/2} \quad (25)$$

$$H_2 = H_1 - Z_{I,1} + Z_{I,2} \quad (26)$$

Further explanation of variables is contained in the nomenclature section.

Cooper<sup>23</sup> has formulated an alternative calculation of substitute source energy release rate and position below the ceiling that provides for generalization to situations in which portions of the time averaged plume flow in the lower layer are at temperatures below the upper layer temperature. In these cases, only part of the plume flow may penetrate the upper layer sufficiently to impact on the ceiling. The remaining portion at low temperature may not penetrate into the hotter upper layer. In the extreme, when the maximum temperature in the lower layer plume flow is less than the upper layer temperature, none of the plume flow will penetrate significantly into the upper layer. This could be the case during the decay phases of an enclosure fire, when the energy release rate is small compared to earlier times in the fire growth and spread. In this calculation of substitute fire source quantities, the first step is to calculate the fraction of the plume mass flow penetrating the upper layer,  $m_2^*$ , from Equations 27 and 28.

$$m_2^* = \frac{1.04599\sigma + 0.360391\sigma^2}{1 + 1.37748\sigma + 0.360391\sigma^2} \quad (27)$$

where

$$\sigma = [\xi/(\xi - 1)] \{ (1 + C_T (\dot{Q}_{I,1}^*)^{2/3})/\xi - 1 \} \quad (28)$$

Then, analogous to Equations 24, 25, and 26 of the previous method

$$Z_{I,2} = Z_{I,1} \xi^{3/5} (m_2^*)^{2/5} [(1 + \sigma)/\sigma]^{1/3} \quad (29)$$

$$\dot{Q}_{c,2} = \dot{Q}_{c,1} [\sigma m_2^*/(1 + \sigma)] \quad (30)$$

$$H_2 = H_1 - Z_{I,1} + Z_{I,2} \quad (31)$$

After the substitute values of energy release rate and distance to the ceiling are calculated, the warm upper layer gas temperature and density are used in the previous correlations developed for ceiling jet flows in uniform ambient environments to predict ceiling jet temperature and velocity values.

Using a substitute fire source technique and a series of steady fires to represent growing fires in an enclosure, Evans has calculated the effects of warm upper layer depth on temperatures in the ceiling jet in an analysis of detector response in compartments.<sup>22</sup>

To demonstrate the use of the techniques, the previous example in which a sofa was imagined to be burning in a showroom may be expanded. Let all the parameters of the problem remain the same except that at 200 s after ignition ( $t - t_i = 120$  s), when the fire energy release rate has reached 2.5 MW, a quiescent warm layer of gas at a temperature of 50°C is assumed to have accumulated under the ceiling to a depth of 2 m. For this case, the two-layer analysis is needed to determine the ceiling jet maximum temperature at the same position as calculated previously (4 m radially distant from the plume impingement point on the ceiling).

All of the two-layer calculations presented assume quasi-steady conditions. Using Equation 18 and the values of parameters in the single-layer calculation, it can be shown that  $\Delta T_2 = 0.85 \Delta T_0$ . So in the uniform ambient case, the quasisteady analysis should be adequate. It will be assumed that this finding will carry over to the two-layer case.

Using Equations 23 through 26 from the work of Evans,<sup>22</sup> values of the energy release rate and position of the substitute fire source which compensates for the two-layer

effects on the plume flow can be calculated. The dimensionless energy release rate of the fire source evaluated at the position of the upper and lower layer interface is

$$\dot{Q}_{I,1}^* = \dot{Q}/(\rho_\infty C p_\infty T_\infty g^{1/2} Z_{I,1}^{5/2})$$

For an actual energy release rate of 2500 KW, ambient temperature of 293 K, and distance between the fire source and an interface between the lower and upper layers of 3 m this becomes

$$\begin{aligned}\dot{Q}_{I,1}^* &= 2500/(1.204 * 1 * 293 * 9.8^{1/2} * 3^{5/2}) \\ &= 0.1452\end{aligned}$$

Using the ratio of upper-layer temperature to lower-layer temperature  $\xi = 323/293 = 1.1024$  and the constant  $C_T = 9.115$ , the dimensionless energy release for the substitute fire source is

$$\dot{Q}_{I,2}^* = 0.1179.$$

Using the value for the constant  $\beta^2 = 0.913$ , the position of the substitute fire source relative to the interface is

$$Z_{I,2} = 3.161$$

Using Equations 25 and 26, the dimensional energy release rate and position relative to the ceiling are found to be

$$\dot{Q}_2 = 2313 \text{ kW}$$

$$H_2 = 5.161 \text{ m}$$

The analogous calculations for substitute fire-source energy release rate and position following the analysis of Cooper<sup>23</sup> Equations 27 through 31 are

$$T = 23.60 \quad m_2^* = 0.962 \quad Z_{I,2} = 3.176$$

so

$$\dot{Q}_2 = 2308 \text{ kW}$$

$$H_2 = 5.176 \text{ m}$$

These two results are essentially identical for the purpose of ceiling jet flow analysis.

The dimensionless maximum temperature in the ceiling jet flow, 4 m from the impingement point, is calculated from Equation 6, using the ceiling height above the substitute source as

$$\Delta T_0^* = [0.188 + 0.313(4/5.161)]^{-4/3}$$

$$\Delta T_0^* = 3.076$$

Using the corresponding energy release rate for the substitute source and the upper layer ambient temperature, the dimensional temperature elevation at the position in the ceiling jet is

$$\begin{aligned}\Delta T &= \Delta T_0^* T_\infty (\dot{Q}_0^*)^{2/3} \\ &= 3.076 * 323 * [2313 / (1.092 * 1 * 323 * 9.8^{1/2} * 5.161^{5/2})]^{2/3}\end{aligned}$$

$$\Delta T = 106 \text{ K}$$

$$T = 106 \text{ K} + 323 \text{ K} = 429 \text{ K} = 156^\circ\text{C}$$

This is 52°C above the temperature calculated previously using the quasi-steady analysis and a uniform 20°C ambient.

## TRANSIENT CEILING JETS

At the beginning of a fire, the initial buoyant flow from the fire must spread across the ceiling, driven by buoyancy, to penetrate the cooler ambient air ahead of the flow. Research studies designed to quantify the temperatures and velocities of this initial spreading flow have only recently been started.<sup>24</sup> At a minimum, it is useful to become aware of the many fluid mechanical phenomena embodied in a description of the ceiling jet flow in a corridor up to the time when the ceiling jet is totally submerged in a quiescent warm upper layer. Borrowing heavily from a description of this flow provided by Zukoski *et al.*,<sup>24</sup> the process is as follows.

A fire starts in a small room with an open door to a long corridor having a small vent near the floor at the opposite end. As the fire starts, smoke and hot gases rise to form a layer near the fire room ceiling. The layer is contained in the small room by the door soffit. [See Figure 2-4.4, part (a).] As the fire continues, hot gas from the room begins to spill out under the soffit into the hallway. The fire grows to a relatively constant energy release rate.

The outflowing gas forms a short, buoyant plume [see Figure 2-4.4, part (b)] that impinges on the hallway ceiling, producing a thin jet that flows away from the fire room in the same manner as the plume within the room flows over the interior ceiling. The gas flow in this jet is supercritical, analogous to the shooting flow of liquids over a weir. The velocity of the gas in this flow is greater than the speed of gravity waves on the interface between the hot gas and the cooler ambient air. The interaction of the leading edge of this flow with the ambient air ahead of it produces a hydraulic jump-like condition, as shown in Figure 2-4.4, part (c). A substantial amount of ambient air is entrained at this jump. Downstream of the jump, the velocity of the gas flow is reduced and mass flow is increased due to the entrainment at the jump. A head is formed at the leading edge of the flow. Mixing between this ceiling-layer flow and the ambient cooler air occurs behind this head.

The flow that is formed travels along the hallway ceiling [see Figures 2-4.4, part (c) and 2-4.4, part (d)] with constant velocity and depth until it impinges on the end wall [see Figure 2-4.4, part (e)]. A group of waves are reflected back toward the jump near the fire room, traveling on the interface. Mixing occurs during the wall impingement process [see Figure 2-4.4, part (f)], but no significant entrainment occurs during the travel of the nonbreaking reflected wave. When these waves reach the jump near the fire room door, the jump is submerged in the warm gas layer, eliminating the entrainment of ambient lower layer air at this position. [See Figure 2-4.4, part (g).] After several wave reflections up and down the corridor along the interface, the wave motion dies out, and a ceiling layer more uniform in depth is produced. This layer slowly grows deeper as the hot gas continues to flow into the hallway from the fire room.

It is clear from this description that quantification of effects in the transient ceiling jet flow is quite complex.

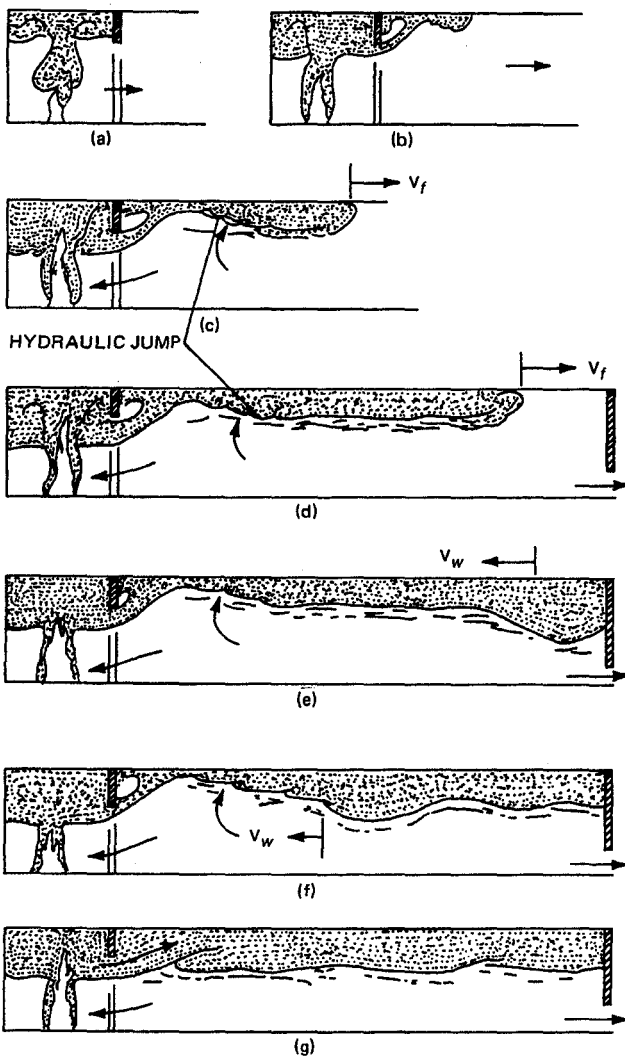


Fig. 2-4.4. Transient ceiling jet flow in a room and corridor.<sup>24</sup>

Analysis and experiments are under way to understand better the major features of a ceiling jet flow in a corridor.<sup>25,26</sup>

## SUMMARY

Reliable means are available to predict the temperatures and velocities of gases in fire-driven ceiling jet flows beneath unobstructed ceilings for both steady and  $t^2$  fire growth. These predictive methods apply to quantifying the maximum temperature and maximum velocity at a given position in the ceiling jet flow and apply to situations where the flow can be considered unconfined. These methods are the basis for acceptable design methods exemplified by Appendix B of NFPA 72, *National Fire Alarm Code*.<sup>19</sup>

## NOMENCLATURE

$A$	$g/(c_p T_\infty \rho_\infty)$
$c_p$	heat capacity at constant pressure
$C_T$	constant related to plume-flow value 9.115 <sup>14</sup>
$g$	gravitational acceleration
$H$	ceiling height above fire source

$m_2^*$	fraction of the fire-plume mass flux penetrating upper layer
$\dot{Q}$	total energy release rate
$Q^*$	$Q/\rho_\infty c_p T_\infty g^{1/2} H^{5/2}$
$r$	radial distance
$t$	time
$T$	gas temperature
$\Delta T$	$T - T_\infty$
$U$	gas velocity
$z$	distance above fire source
$\alpha$	fire growth parameter for $t^2$ fires
$\beta^2$	constant related to plume flow value 0.913 <sup>14</sup>
$\rho$	gas density
$\xi$	ratio of temperatures $T_{\infty,2}/T_{\infty,1}$
$\sigma$	parameter defined in Equation 16

## Subscripts

0	based on steady fire
1	lower layer
2	upper layer
$\infty$	ambient, outside ceiling jet or plume flows
$c$	convective fraction
$f$	associate with gas travel delay
$l$	value at the interface position between the warm upper layer and cool lower layer
$i$	reference value at ignition

## Superscripts

*	dimensionless quantity
---	------------------------

## REFERENCES CITED

1. R.W. Pickard, D. Hird, and P. Nash, *F.R. Note 247*, Building Research Establishment, Borehamwood (1957).
2. P.H. Thomas, *F.R. Note 141*, Building Research Establishment, Borehamwood (1955).
3. R.L. Alpert, *Fire Tech.*, 8, 181 (1972).
4. R.L. Alpert, *Comb. Sci. and Tech.*, 11, 197 (1975).
5. H.Z. You, *Fire and Mats.*, 9, 46 (1985).
6. G. Heskestad and T. Hamada, *FMRC J.I. OKOELRU 070(A)*, Factory Mutual Research Corp., Norwood (1984).
7. L.Y. Cooper, NBSIR 87-3535, *J. of Heat Trans.*, 104, 446 (1982).
8. L.Y. Cooper and A. Woodhouse, *J. of Heat Trans.*, 108, 822 (1986).
9. H.Z. You and G.M. Faeth, *Fire and Mats.*, 3, 140 (1979).
10. C.C. Veldman, T. Kubota, and E.E. Zukoski, *NBS-GCR-77-97*, U.S. National Bureau of Standards, Gaithersburg (1977).
11. E.E. Zukoski and T. Kubota, *NBS-GCR-77-98*, National Bureau of Standards, Gaithersburg (1977).
12. V. Motevalli and C.H. Marks, "Characterizing the Unconfined Ceiling Jet under Steady-State Conditions: A Reassessment," *Fire Safety Science Proceedings of the 3rd International Symposium*, G. Cox and B. Langford, eds., Elsevier Applied Science, New York, 301 (1991).
13. D.D. Evans and D.W. Stroup, *Fire Tech.*, 22, 54 (1986).
14. E.E. Zukoski, T. Kubota, and B. Cetegen, *F. Safety J.*, 3, 107 (1981).
15. G. Heskestad and M.A. Delichatsios, *The Initial Convective Flow in Fire*, 17th International Symposium on Combustion, Combustion Institute, Pittsburgh (1978).
16. C.L. Beyler, *F. Safety J.*, 11, 53 (1986).
17. R.P. Schifilliti, *Use of Fire Plume Theory in the Design and Analysis of Fire Detector and Sprinkler Response*, Thesis, Worcester Polytechnic Institute (1986).
18. G. Heskestad and M.A. Delichatsios, *NBS-GCR-77-86 and NBS-GCR-77-95*, National Bureau of Standards, Gaithersburg (1977).

19. NFPA 72, *National Fire Alarm Code*, National Fire Protection Association, Quincy, MA (1993).
20. M.A. Delichatsios, *Comb. and Flame*, 43, 1 (1981).
21. D.D. Evans, *Comb. Sci. and Tech.*, 40, 79(1984).
22. D.D. Evans, *F. Safety J.*, 9, 147 (1985).
23. L.Y. Cooper, *A Buoyant Source in the Lower of Two, Homogeneous, Stably Stratified Layers*, 20th International Symposium on Combustion, Combustion Institute, Pittsburgh (1984).
24. E.E. Zukoski, T. Kubota, and C.S. Lim, *NBS-GCR-85-493*, National Bureau of Standards, Gaithersburg (1985).
25. H.W. Emmons, "The Ceiling Jet in Fires," *Fire Safety Science, Proceedings of the 3rd International Symposium*, G. Cox and B. Langford, eds., Elsevier Applied Science, New York, 249 (1991).
26. W.R. Chan, E.E. Zukowski, and T. Kubota, "Experimental and Numerical Studies on Two-Dimensional Gravity Currents in a Horizontal Channel," NIST-GCR-93-630, National Institute of Standards and Technology, Gaithersburg (1993).